Constraining the flavor changing Higgs couplings to the top-quark at the LHC

David Atwood,[a] **Sudhir Kumar Gupta**[b] **and Amarjit Soni**[c]

[a]*Dept. of Physics and Astronomy, Iowa State University,*
Ames, IA 50011, U.S.A.

[b]*ARC Centre of Excellence for Particle Physics at the Terascale,*
School of Physics, Monash University, Melbourne, Victoria 3800 Australia

[c]*Theory Group, Brookhaven National Laboratory,*
Upton, NY, 11973, U.S.A.

E-mail: atwood@iastate.edu, Sudhir.Gupta@monash.edu,
adlersoni@gmail.com

ABSTRACT: We study the flavor-changing couplings of the Higgs-boson with the top-quark using the processes: (a) $pp \longrightarrow tt$, (b) $pp \longrightarrow \bar{t}j$, and, (c) $pp \longrightarrow \bar{t}jh$ at the LHC in light of current discovery of a 126 GeV Higgs-Boson. Sensitivities for the flavor-changing couplings are estimated using the LHC data that was collected until spring 2013. It is found that the process (c) is the most capable of yielding the best upper bound on the flavor-changing couplings with 2σ level sensitivities of $|\xi_{tc}^2 + \xi_{tu}^2|^{1/2} \lesssim 7.3 \times 10^{-3}$ and $\lesssim 2.9 \times 10^{-3}$ resulting from $t \to bl\nu_l, h \to jj$ with the 7 TeV and 8 TeV centre-of-mass energies respectively using existing data from the LHC. The corresponding bounds from $h \to b\bar{b}$ are worse by a factor of about 1.8.

KEYWORDS: Higgs Physics, Beyond Standard Model, Phenomenological Models

ARXIV EPRINT: 1305.2427

Contents

1 Introduction

Last year the ATLAS and the CMS experiments at the LHC made a monumental discovery, namely that of a scalar resonance with mass of about 126 GeV and properties akin to that of a Standard Model (SM) Higgs boson [1, 2]. By now all of the prominent decay modes that have been measured are found to be quite consistent within appreciable errors with expectations based on the SM [3, 4].

Given that this particle is of such a fundamental importance it should be clear that we need to study all its properties to excruciating details. In particular, we have to understand the issue of its stability against radiative corrections. Naively, one expects new physics to be there around a few TeV scale. To decipher its nature we are likely to need very precise measurements of the couplings of the Higgs.

In this work we will address the flavor changing couplings involving the Higgs and the top-quark and try to use data to constrain these couplings. As is well known within the SM, such flavor off-diagonal couplings are highly suppressed and occur only at loop level. At least in some popular models, such as warped extra-dimension the Higgs and the top-quark may be particularly sensitive to flavor changing effects as both of them are localized close to the TeV brane and the profiles of the KK-gluons are also peaked there

[5–13]. We study several different processes involving the top-quark and the Higgs and find that $pp \longrightarrow \bar{t}jh$, (where j is a jet), is very sensitive in providing stringent constraints.

In warped models of course there are also general expectations of extra CP violating phases of $\mathcal{O}(1)$. So CP violation studies are also highly motivated and we will return to this in another publication.

If such FCNCs are present, depending upon their size, they can influence the top-induced production processes, such as the single-top production processes where the top-quark is produced in association with lighter quarks, and Higgs, it can also modify (1) decay of the top-quark by allowing its decays into the Higgs-boson and a charm or an up-quark in addition to its known decays within the SM, and, (2) decay of the Higgs-boson into a virtual top-quark in association with a charm or an up-quark where the virtual top-decays as in (1).

The organisation of the paper is following: we begin with a brief introduction to the flavor-changing operators. In sections 3 and 4 we will discuss decays of the Higgs boson and the top-quark, and the production processes we propose in this article. In section 5 we will present the actual analysis of the proposed processes in the light of LHC data on the Higgs-boson and the pre-existing data on the top-quark from the Tevatron experiment. Finally we summarise our findings in section 6.

2   The flavor-changing top-quark couplings

When the flavor-changing couplings of the Higgs are present, the SM Lagrangian can be extended by allowing the following additional terms,

$$\mathcal{L}_{\text{flavor}}^h = \xi_{tc}\bar{t}cH + \xi_{tu}\bar{t}uH + h.c., \tag{2.1}$$

where for now, we consider that the flavor-changing couplings, ξ_{tu}, and, ξ_{tc} are real and symmetric, i.e. $\xi_{tq_u} = \xi_{tq_u}^\dagger = \xi_{q_u t} = \xi_{q_u t}^\dagger$, where, $q_u = u, c$. As mentioned before, CP studies will be dealt with in a later study.

It is to be noted here that similar flavor-changing Lagrangian has been also widely studied in the refs. [14–20], for example. These FV-interactions allow some interesting phenomenological consequences which are as follows:

(A) At the decay level:

1. In addition to the usual decay modes, Higgs can also decay into single $W^{\pm}$-boson via an off-shell top, e.g. $h \to \bar{q}_u(t^* \to bW^+)$; $(q_u = u, c)$ where '*' means off-shell top,

2. top-quark can now also decay into a charm or an up-quark and a Higgs, e.g. $t \to q_u h$.

(B) At the production level:

1. Because of FCNC we can have a pair of same-sign top produced via t-channel exchange of the Higgs, e.g. $pp \to tt(\bar{t}\bar{t})$ through the parton level subprocesses, $uu \to tt$, $uc \to tt$ and $cc \to tt$.

2. The FCNCs of Higgs can contribute significantly to the production processes where a top-quark is produced in association with light partons, e.g. $pp \to t\bar{j}_u(\bar{t}j_u)$, where $j_u = u, c$.

3. Higgs can now be produced in association with a top-quark and an up or a charm quark, e.g. the process $pp \to t\bar{c}h(\bar{t}ch)$.

Let us discuss their consequences one-by-one in the following sections.

3 Higgs boson and top-quark decay rates

Let us now consider the decays of top-quark and Higgs-boson in the following subsections.

3.1 Top quark decays

Because $m_t - m_h > m_c, m_u, m_b$, in addition to the usual decay into a bottom quark and a W^+ Boson, the top-quark can also decay into a charm (or an up) quark and a Higgs-Boson. Therefore, the total decay width of the top-quark, Γ_t will take the following form,

$$\Gamma_t = \Gamma_{t \to bW^+} + \Gamma_{t \to ch} + \Gamma_{t \to uh}. \tag{3.1}$$

The $t \longrightarrow bW^+$ decay width at the NLO level is given by [21, 22],

$$\Gamma_{t \to bW^+} = \frac{G_F m_t^3}{8\sqrt{2}\pi} \left[1 - \frac{2\alpha_s}{3\pi} \left(\frac{2\pi^2}{3} - \frac{5}{2} \right) \right] \left(1 - \tau_W^2 \right)^2 \left(2\tau_W^2 + 1 \right) \tag{3.2}$$

The $t \longrightarrow q_u h$ $(q_u = u, c)$ partial decay width is given as,

$$\Gamma_{t \to q_u h} = \frac{\xi_{tq_u}^2 m_t}{16\pi} \left[(\tau_{q_u} + 1)^2 - \tau_h^2 \right] \sqrt{1 - (\tau_h - \tau_{q_u})^2} \sqrt{1 - (\tau_{q_u} + \tau_h)^2} \tag{3.3}$$

where, $\tau_W = \frac{M_W}{m_t}$, $\tau_h = \frac{M_h}{m_t}$, $\tau_{q_h} = \frac{m_{q_h}}{m_t}$. Using the measured values of G_F, α_s, M_W, M_h etc., we obtain,

$$\Gamma_t = \Gamma_t^{SM} + [0.8\ \xi_{tc}^2 + 0.78\ \xi_{tu}^2]\ \text{GeV}, \tag{3.4}$$

where $\Gamma_t^{SM} = 2 \pm 0.7\,\text{GeV}$ [22] and $\Gamma_t^{SM} \equiv \Gamma_{t \to bW^+}^{SM}$.

From the above expression it is clear that the maximum deviation in the $Br(t \to bW^+)$ from the SM corresponds to the $\xi_{tc} = 1 = \xi_{tu}$ and amounts to be about 41%. As we will show later in this paper, the current LHC data constraints on these FCNCs will be much stronger, i.e. $\lesssim 10^{-3}$. To put things into perspective, in the SM, the diagonal couplings of the top-quark and the charm-quark $y_{t,c} = \frac{\sqrt{2}m_{t,c}}{v}$; $v = 246\,\text{GeV}$ being the vaccum-expectation value, are $y_t \simeq 1$ and $y_c \simeq 0.008$ respectively.

3.2 Decays of the Higgs-Boson

Because of the flavor-changing couplings endowed by eq. (2.1) the Higgs-Boson can also have the following three-body decays:

$h \to q_u(\bar{t}^* \to \bar{b}W^-)$, $h \to \bar{q}_u(t^* \to bW^+)$; ($q_u = u, c$) where '*' means off-shell top. Using CalcHep [23] we numerically estimate,

$$\Gamma_{h \to q_u(\bar{t}^* \to \bar{b}W^-)} \simeq 0.28\xi_{tq_u}^2 \text{ MeV}. \tag{3.5}$$

Therefore the total width, Γ_h would be,

$$\Gamma_h = \Gamma_h^{SM} + \sum_{q_u} \Gamma_{h \to q_u(\bar{t}^* \to \bar{b}W^-)} + \Gamma_{h \to \bar{q}_u(t^* \to bW^+)}$$
$$\simeq \left[\Gamma_h^{SM} + 0.56\left(\xi_{tc}^2 + \xi_{tu}^2\right)\right] \text{ MeV}, \tag{3.6}$$

where $\Gamma_h^{SM} = 3.3$ using CalcHep.

In our model the usual two-body decays of the Higgs boson, i.e., the LHC Higgs observables would take the following form,

$$\mathcal{R}_{ggX} = \frac{\sigma_{gg \to h}}{\sigma_{gg \to h}^{SM}} \cdot \frac{\mathcal{BR}(h \to X)}{\mathcal{BR}^{SM}(h \to X)} \simeq \frac{\Gamma_{h \to gg}}{\Gamma_{h \to gg}^{SM}} \cdot \left(\frac{\Gamma_{h \to X}}{\Gamma_h}\right) \Big/ \left(\frac{\Gamma_{h \to X}^{SM}}{\Gamma_h^{SM}}\right) \simeq \frac{\Gamma_h^{SM}}{\Gamma_h}; \quad (3.7)$$

where, X stands for two-body decay products of the produced Higgs-Boson, e.g. $X = \gamma\gamma, b\bar{b}, WW^*, ZZ^*, \tau^+\tau^-$ etc. In the equation above, we have assumed that $\frac{\sigma_{gg \to h}}{\sigma_{gg \to h}^{SM}} = \frac{\Gamma_{gg \to h}}{\Gamma_{gg \to h}^{SM}} \simeq 1$ which is due to the fact that the flavor-changing couplings discussed in our paper affect the $gg \to h$ production process at the next-loop level and therefore the effects are expected to be much smaller.

4 Production processes at the LHC

We now turn to study some interesting production processes where the effect of the afore-mentioned flavor-changing couplings could be significant. Obviously the very first process, the $t\bar{t}$ may not be suitable when both the produced tops decay through their ususal SM decay model as it will have relatively large SM background. Among the other leading processes are:

- (a) the same-sign top-pair, e.g. $pp \to tt(\bar{t}\bar{t})$,

- (b) processes where a top-quark is produced in association with a light jet, e.g. $pp \to t\bar{j}_u(\bar{t}j_u)$, where $j_u = u, c$, and,

- (c) processes where the top-quark is produced in association with a Higgs and a light jet, e.g. $pp \to t\bar{j}_uh(\bar{t}j_uh)$.

The process (a), the same-sign top pair production is an interesting one as it has very little SM background. In a recent work by us [24], it was found that this process can play a very important role in excluding many models proposed to explain the forward-backward

asymmetry of the top-quark $A^t_{\rm FB}$ as observed by the Tevatron experiments (Also see, for example, [25–27]). Within the model under consideration in this paper, at the LHC, a pair of same-sign top pair can be produced via the t-channel exchange of the Higgs through two flavor-changing couplings. For the $m_h = 125.7\,\text{GeV}$, the bare cross-sections for this process is given by the following equations:

$$\sigma(pp \to tt) = 49.5\xi^4_{tu} + 13.6\xi^2_{tc}\xi^2_{tu} + 0.3\xi^4_{tc} \text{ pb (at } \sqrt{s} = 7 \text{ TeV}),$$
$$\sigma(pp \to tt) = 56.2\xi^4_{tu} + 17.7\xi^2_{tc}\xi^2_{tu} + 0.4\xi^4_{tc} \text{ pb (at } \sqrt{s} = 8 \text{ TeV}), \qquad (4.1)$$

respectively.

In eqs. above we notice that the numerical factors for the ξ^4_{tu} is larger than those proportional to $\xi^2_{tc}\xi^2_{tu}$ and ξ^4_{tc}. This is because of the fact that the first term is due to the scattering of two valence up-quarks as opposed to other terms where one or both the initial partons are the (sea-)charm-quark(s). As discussed in refs. [24] and in [28] this process has very little SM background and hence can be useful in constraining the couplings ξ_{tc} and ξ_{tu}. We will discuss this in detail in the next section.

The other two processes namely, (b) and (c) are perhaps even more interesting as both of these occur via only one flavor-changing vertex unlike the process (a). Therefore, we expect the cross-sections for these processes to be proportional to $a\xi^2_{tu} + b\xi^2_{tc}$ where a and b are arbitrary constants.

More specifically, the processes where a top or anti-top quark is produced in association with an up, anti-up, charm or anti-charm quark can occur via two ways: one, where a pair of initial (anti-)quarks with same or different flavor undergo t-channel exchange through the Higgs, e.g. processes of the form $qq_u \to tq$ and $q\bar{q}_u \to \bar{t}q$, where, $q = \{q_u, b\}$, $q_u = \{u, c\}$. Therefore we expect cross-sections for these subprocesses to be proportional to $y^2_q \xi^2_{tq_u}$ where y_q is the Yukawa coupling of the quark q. This suggests that although at the subprocess level, we gain in the processes where the initial parton is a b or a $\bar{b}$ due to large value of y_b compared to y_c and y_u at the proton-proton level, we may loose due to relatively smaller parton densities for the b-quarks. The other type of contribution is due to the off-shell Higgs production in the s-channel due to gluon-pair fusion, where the Higgs decays into $t\bar{q}_u$ or $\bar{t}q_u$. The composition of this process is discussed in detail for $m_h = 125.7\,\text{GeV}$ in the appendix A. The corresponding background and the total cross-sections for $\sqrt{s} = 7$ and 8 TeV are summarised in table 1. The major source for this process is production of $t\bar{b}(\bar{t}b)$ mediated by an off-shell $W^\pm$ in the s-channel.

The production process (c) requires production of a $t\bar{t}$ pair where one of the top decays into a Higgs and an up or charm-quark, or it can also take place via the pair production processes $u\bar{u}$ and $c\bar{c}$ where one of the off-shell up or charm goes into a top and a Higgs (see figure 1). This process has very little SM background due to the production of (i) $t\bar{b}Z(\bar{t}bZ)$, and, (ii) $t\bar{b}h(\bar{t}bh)$. Clearly both of these processes are electro-weak processes which are mediated by an off-shell $W^\pm$-boson. e.g., $pp \to W^{\pm*}Z(W^{\pm*}h)$, and $W^* \to t\bar{b}(\bar{t}b)$. Therefore we expect to find better bounds on ξ_{tc} and ξ_{tu} using this process. A detail of the cross-sections and corresponding background to this process is given in table 2.
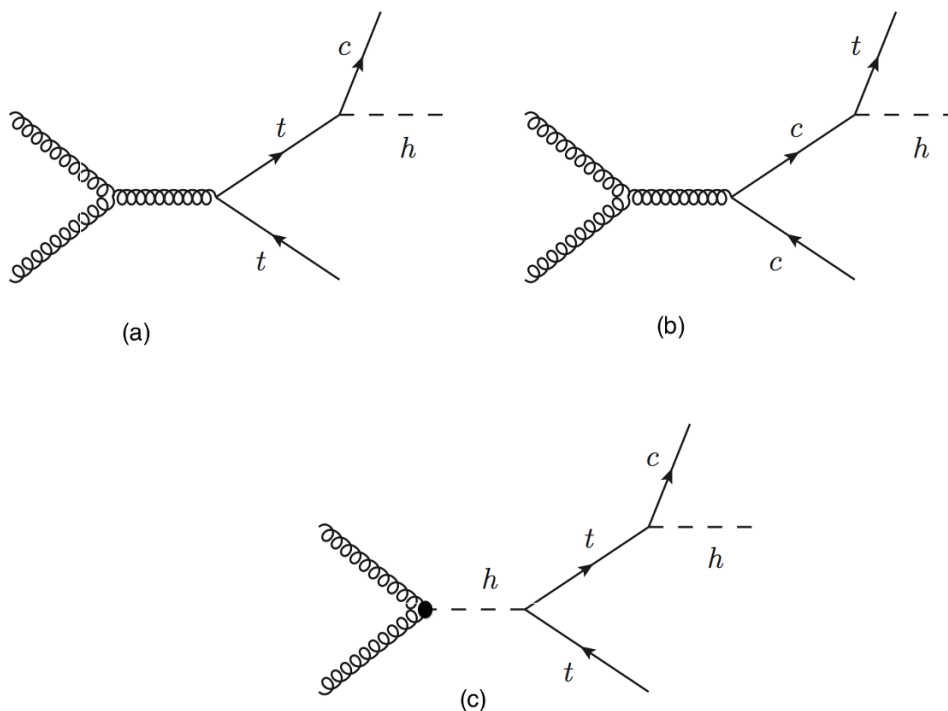
Figure 1. Representative s-channel Feynman diagrams for the partonic process $gg \rightarrow tch$.

Serial Number	Process	LHC-7	LHC-8
(1)	$pp \longrightarrow t\bar{c}(\bar{t}c, tc, \bar{t}\bar{c})$	$42.06\xi_{tc}^2 + 4.81\xi_{tu}^2$	$59.7\xi_{tc}^2 + 5.44\xi_{tu}^2$
(2)	$pp \longrightarrow h \longrightarrow t\bar{c}(\bar{t}c)$	$41.2\xi_{tc}^2$	$58.52\xi_{tc}^2$
(3)	$pp \longrightarrow t\bar{u}(\bar{t}u, tu, \bar{t}\bar{u})$	$0.4\xi_{tc}^2 + 44.54\xi_{tu}^2$	$0.61\xi_{tc}^2 + 59.67\xi_{tu}^2$
(4)	$pp \longrightarrow h \longrightarrow t\bar{u}(\bar{t}u)$	$41.2\xi_{tu}^2$	$58.52\xi_{tu}^2$
(1) + (3)	$pp \longrightarrow tq_u(\bar{t}q_u)$	$42.46\xi_{tc}^2 + 49.35\xi_{tu}^2$	$60.31\xi_{tc}^2 + 65.11\xi_{tu}^2$
SM Background	$pp \longrightarrow t\bar{b}(\bar{t}b, tj, \bar{t}j, tjj, \bar{t}jj)$	43.49×10^3	56.17×10^3

Table 1. Single top production cross-section (in fb units) at the LHC for $\sqrt{s} = 7$ and $8\,\mathrm{TeV}$ in association with an up or a charm (anti-)quark. In all the processes the implemented basic cuts on the associated (anti-)quark are as follows: $p_T = 25\,\mathrm{GeV}$, and, $|\eta| \leq 2.7$. The Yuwaka couplings y_u, y_c, y_t have been estimated using $m_u = 3\,\mathrm{MeV}$, $m_c = 1.44\,\mathrm{GeV}$ and $m_t = 172.4\,\mathrm{GeV}$ respectively. The Higgs-Boson mass has been set to the observed central value, $m_h = 125.7\,\mathrm{GeV}$.

5 Flavor-changing Higgs and LHC observations

In this section we will first discuss the flavor-changing couplings ξ_{tc} and ξ_{tu} in the context of the individual experimental observations as listed in table 3 and later we will make use of them all in order to obtain constraints on these couplings using the processes we propose here. We will also discuss the projected sensitivities of the aforementioned couplings in the context of 14 TeV data in the second subsection.

Serial Number	Process	LHC-7	LHC-8
(5)	$pp \longrightarrow t\bar{c}h(\bar{t}ch, tch, \bar{t}\bar{c}h)$	$75.25 \times 10^3\xi_{tc}^2$	$107.99 \times 10^3\xi_{tc}^2$
(6)	$pp \longrightarrow t\bar{u}h(\bar{t}uh, tuh, \bar{t}\bar{u}h)$	$79.21 \times 10^3\xi_{tu}^2$	$112.76 \times 10^3\xi_{tu}^2$
(5) + (6)	$pp \longrightarrow t\bar{q}_u h(\bar{t}q_u h)$	$(75.25\xi_{tc}^2 + 79.21\xi_{tu}^2) \times 10^3$	$(107.99\xi_{tc}^2 + 112.76\xi_{tu}^2) \times 10^3$
SM Background	$pp \longrightarrow t\bar{b}Z(\bar{t}bZ)$	2.54 (1.07)	3.32 (1.39)
	$pp \longrightarrow t\bar{t} + nj; n \le 3$	176.6×10^3	261.5×10^3
	$pp \longrightarrow t\bar{t} + b\bar{b} + nj; n \le 3$	716.9	1175.6
	$pp \longrightarrow t\bar{b}h(\bar{t}bh)$	0.54 (0.23)	0.7 (0.29)

Table 2. Single top production cross-section (in fb units) at the LHC for $\sqrt{s} = 7$ and $8\,\mathrm{TeV}$ in association with an up or a charm (anti-)quark and a Higgs-Boson. In all the processes the implemented basic cuts and all other SM parameters are same as given in table 1.

Observable	Value	Experiment
Γ_t	$2 \pm 0.7\,\mathrm{GeV}$	Tevatron [22]
m_h	$125.5 \pm 0.2\,\mathrm{(stat)}^{+0.5}_{-0.6}\,\mathrm{(sys)}\,\mathrm{GeV}$	ATLAS [3]
	$125.8 \pm 0.5\,\mathrm{(stat)} \pm 0.2\,\mathrm{(sys)}\,\mathrm{GeV}$	CMS [4]
	$125.7 \pm 0.4\,\mathrm{GeV}$	Combined
$\mathcal{R}_{gg\gamma\gamma}$	$1.65^{+0.34}_{-0.30}$	ATLAS [29, 30]
	$1.11^{+0.32}_{-0.30}$	CMS [31, 32]
	1.36 ± 0.23	Combined
$\mathcal{R}_{gg2l2\nu}$	1.01 ± 0.31	ATLAS [33, 34]
	$0.76^{+0.21}_{-0.21}$	CMS [35, 36]
	0.84 ± 0.17	Combined
$\mathcal{R}_{gg4l}$	$1.7^{+0.5}_{-0.4}$	ATLAS [29, 37]
	$0.91^{+0.30}_{-0.24}$	CMS [35, 38]
	1.12 ± 0.26	Combined
$D0$-oscillations	$|\xi_{tu}\xi_{tc}| < 0.9 \times 10^{-3}$	UTfit Collaboration [39]

Table 3. Measured values of various observables used in our analysis; combined here means weighted average of ATLAS and CMS values for a given observable.

5.1 Flavor changing couplings at the LHC-7 and LHC-8

Let us first begin with total decay width of the top-quark, Γ_t. As we have already noticed in section 3.1, Γ_t receives positive contributions proportional to ξ_{tu}^2 and to ξ_{tc}^2 due to additional decay processes $t \to uh$ and $t \to ch$ respectively.

This gives an upper bound on the $\sqrt{\xi_{tc}^2 + \xi_{tu}^2}$ of about 1.3 at the 2σ level which is quite mild.

In a similar way we study the Higgs observables $\mathcal{R}_{gg\gamma\gamma}$, $\mathcal{R}_{gg2l2\nu}$, $\mathcal{R}_{gg4l}$ and their combined effects in light of recently updated data during Moriond-2013 as discussed in table 3.
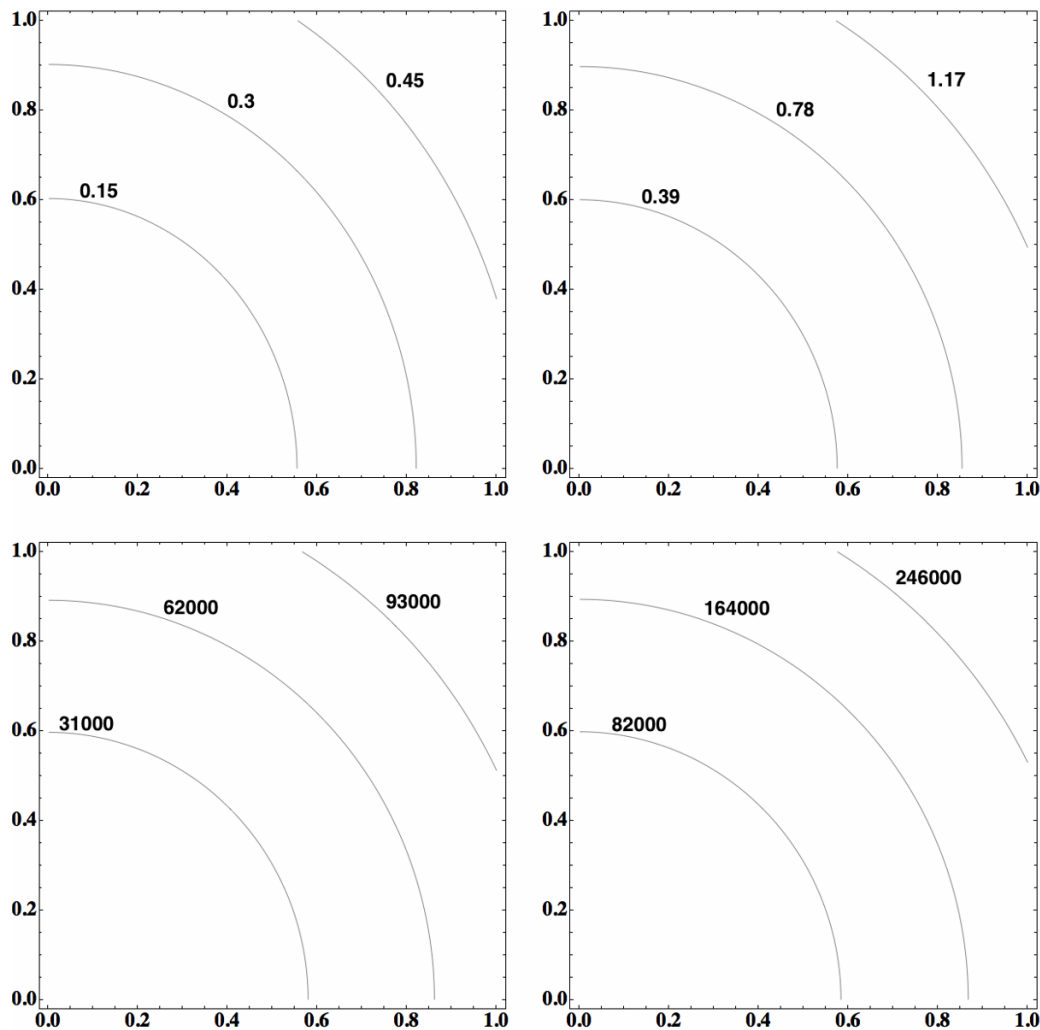
Figure 2. Contour plots in $\xi_{tc} - \xi_{tu}$ plane for signal-significance, $\frac{S}{\sqrt{B}}$, at the production level, for the processes $pp \longrightarrow t\bar{j}_u(\bar{t}j_u)$ (top) and $pp \longrightarrow t\bar{j}_u h(\bar{t}j_u h)$ (bottom) for $\sqrt{s} = 7$ (left) and 8 TeV (right) data at the LHC.

Using the LHC data on various Higgs-observables, one obtains upper bounds on $\sqrt{\xi_{tc}^2 + \xi_{tu}^2}$ of about 1.7, 3.3, 1.8, and, 1.2, for $\mathcal{R}_{gg\gamma\gamma}$, $\mathcal{R}_{gg2l2\nu}$, $\mathcal{R}_{gg4l}$ and for their combined effect respectively. This means the whole range of ξ_{tc} and ξ_{tu} (between -1 to +1) is allowed by these observables at the 2σ level. Note also that the bound that we will obtain later in this paper from $pp \to tch$ will be much stronger, $\lesssim 10^{-3}$.

In order to study the production processes we incorporated flavor-changing couplings in MadGraph5 [40–42]. We evaluate parton densities at a scale $\mu_R = \sqrt{\hat{s}} = \mu_F$ using CTEQ6L1 [43, 44].

We present our result for the $\sqrt{s} = 7$ TeV with an integrated luminosity of $\int \mathcal{L}dt = 5\,\text{fb}^{-1}$ and for $\sqrt{s} = 8$ TeV with $\int \mathcal{L}dt = 22\,\text{fb}^{-1}$ in figures 2 at the bare production level.

Using the formulae for the production cross-sections in our model and their respective SM backgrounds as mentioned in eqs. (4.1) and tables 1 and 2, and the constraints due

to the Γ_t and the LHC Higgs discovery observables $R_{gg\gamma\gamma}$, $R_{gg2l2\nu}$, and, R_{gg4l}, we find the following upper bounds on the $\sqrt{a\xi_{tc}^2 + \xi_{tu}^2}$ at the 2σ level;

$$\sqrt{a\xi_{tc}^2 + \xi_{tu}^2} \lesssim \begin{cases} 0.4 \ (0.2) & \text{for process (a)} \\ 0.9 \ (0.9) & \text{for process (b)} \\ 2.8 \ (1) \times 10^{-3} & \text{for process (c)} \end{cases} \qquad (5.1)$$

for the $\sqrt{s} = 7\,\text{TeV}$ with $5\,\text{fb}^{-1}$ ($\sqrt{s} = 8\,\text{TeV}$ with $22\,\text{fb}^{-1}$) data with $a = 0.08$ for the process (a) and $a = 1$ for processes (b) and (c).

Clearly the bounds due to process (b) are not so promising which is partially due to the fact that it suffers from large SM background as mentioned in table 1. The reason for them being the same for both the 7 TeV and 8 TeV LHC centre-of-mass energies is that it in determining these the combined effect of the constraints on the top-quark decay width and the Higgs observables play a dominant role. Note also that although the processes (a) puts mild bound on $\sqrt{a\xi_{tc}^2 + \xi_{tu}^2}$ it is interesting to analyse because it leads to unique signature in the form of a pair of same-sign leptons. The process (c) is certainly the best process among all of the aforementioned ones as it turns out to be very sensitive even to small values of the flavor-changing couplings.

It is to be noted that in order to obtain the aforementioned bounds, we have assumed that, (1) we will be able to reconstruct the produced (anti-)top-quark(s), and the Higgs boson fully in all its detection modes, and, (2) the number of signal events do not exceed three where the SM background is not significant for the given LHC luminosity. However due to poor reconstruction especially for the cases where the top-quark(s) decays hadronically into a b-jet and a pair of light parton jet, the above limits may not be so realistic. We therefore turn our focus to obtain the detection level bounds on these couplings. For this we work with processes with at least one lepton in the final state. Thus, in all the production processes we allow the produced (anti)top-quark to decay semileptonically, e.g, $t \to bl\nu_l$, where $l = e, \mu$. In case of the process (c) where a Higgs is also produced in association with the top-quark and a jet, we work with $h \to b\bar{b}$, $h \to \gamma\gamma$ and $h \to jj$, where $j = g, q, \bar{q}, b, \bar{b}$. The reason for considering $h \to b\bar{b}$ is merely to gain statistical advantage as within SM the branching ratio for $h \to b\bar{b}$ for the given value of m_h is about 79%. For the case where the Higgs decays into a pair of photons, although the branching ratio is quite suppressed $\simeq 2.9 \times 10^{-3}$, we expect it to be relatively cleaner than the $h \to b\bar{b}$ case.

With this in mind we will therefore have the following topologies:

- $l^\pm l^\pm + 2b-\text{jets} + \displaystyle{\not}E_T$, from the process (a),

- $l^\pm + j + b-\text{jet} + \displaystyle{\not}E_T$, from process (b), and,

- $l^\pm + j + 3b-\text{jets} + \displaystyle{\not}E_T$, when $h \to b\bar{b}$, $l^\pm + j + b-\text{jet} + 2\gamma + \displaystyle{\not}E_T$, when $h \to \gamma\gamma$, and, $l^\pm + 3j + b-\text{jet} + \displaystyle{\not}E_T$, when $h \to jj$, from process (c).

The set of basic cuts used on the photons/leptons/jets in our study are as follows:

$p_{T_{l,j,\gamma}} > 25\,\text{GeV}$, $|\eta_{l,j,\gamma}| < 2.7$, $\Delta R_{kk}, \Delta R_{ik}, > 0.4$, $\displaystyle{\not}E_T > 30\,\text{GeV}$, with $i, k = \{l, j, \gamma\}$. In addition, we also assume a b-jet identification efficiency of 58% ([45], see p. 317–346).

Process	LHC-7	LHC-8
$pp \longrightarrow t\bar{t} + n-$jets	176.64	261.52
$pp \longrightarrow t\bar{t} + b\bar{b} + n-$jets	0.72	1.18
Total	177.36	262.7

Table 4. Other subleading SM backgrounds (in pb) for the production process (c) for $\sqrt{s} = 7$ and 8 TeV.

Process	LHC-7	LHC-8
$pp \longrightarrow t\bar{t} + n-$jets	0.33	0.49
$pp \longrightarrow t\bar{t} + b\bar{b} + n-$jets	0.0014	0.002
Total	0.33	0.49

Table 5. Other subleading SM backgrounds (in pb) for the production process (c) followed by the decays $h \to b\bar{b}$ and $t \to bl\nu_l$ for $\sqrt{s} = 7$ and 8 TeV.

Other SM backgrounds: it is to be noted that because a light parton jet can fake the b-jet with probabilities of about 10% for a charm-jet and about 1% for other light jets respectively [46, 47]), there can be other subleading SM backgrounds for the process (c), particularly when $h \to b\bar{b}$ and $t \to bl\nu_l$. In this catagory, the leading background contribution come from the processes $pp \to t\bar{t} + n-$jets and $pp \to t\bar{t} + b\bar{b} + n-$jets, where n represents number of jets.[1]

Using `MadGraph`, for $n \leq 3$, cross-sections for these processes have been estimated to be $\simeq 177$ pb and $\simeq 0.7$ pb respectively at the $\sqrt{s} = 7$ TeV at the bare level. With the above sets of basic cuts, for our final state $pp \to l^\pm + j + 3b-$jets$+ \not{E}_T$, the requirement that one of the jet pair reconstructs to m_h within 2σ, these aforementioned backgrounds are reduced to 0.33 fb and 0.0014 fb respectively. The corresponding signal rates are reduced by 0.42, 0.57 and 0.43 respectively for the processes $l^\pm + j + 3b-$jets$+ \not{E}_T$, $l^\pm + j + b-$jet$+ 2\gamma + \not{E}_T$, and, $l^\pm + 3j + b-$jet$+ \not{E}_T$. Similar estimates for $\sqrt{s} = 8$ TeV have been summarised in table 4 and 5. Thus our estimates suggest that although at the production level such backgrounds are huge for the LHC integrated luminosities we consider in our analysis, with the aforementioned cuts, these can be reduced to a level where their effects become insignificant for our purposes.

Thus, after combining all the constraints from the Higgs observations and the top-quark decay width, one obtains the following 2σ bounds:

$$\sqrt{a\xi_{tc}^2 + \xi_{tu}^2} \lesssim \begin{cases} 0.8 \ (0.4) & \text{for } pp \to l^\pm l^\pm + 2b-\text{jets} + \not{E}_T \\ 0.9 \ (0.9) & \text{for } pp \to l^\pm + j + b-\text{jet} + \not{E}_T \\ 13 \ (5) \times 10^{-3} & \text{for } pp \to l^\pm + j + 3b-\text{jets} + \not{E}_T \\ 20.6 \ (8.3) \times 10^{-2} & \text{for } pp \to l^\pm + j + b-\text{jet} + 2\gamma + \not{E}_T \\ 7.3 \ (2.9) \times 10^{-3} & \text{for } pp \to l^\pm + 3j + b-\text{jet} + \not{E}_T \end{cases} \qquad (5.2)$$

---

[1]We thank J. Evans for discussion on this background.

with $a = 0.08$ for the process (a) and $a = 1$ for processes (b) and (c), for the $\sqrt{s} = 7\,\mathrm{TeV}$ with $5\,\mathrm{fb}^{-1}$ ($\sqrt{s} = 8\,\mathrm{TeV}$ with $22\,\mathrm{fb}^{-1}$) data. Clearly the process $pp \to l^\pm + 3j + b-\mathrm{jet} + \not{E}_T$ gives the best bound which is about $\mathcal{O}(2.9 \times 10^{-3})$ using the full $8\,\mathrm{TeV}$ data while the corresponding bound for the process $pp \to l^\pm + j + b-\mathrm{jet} + 2\gamma + \not{E}_T$ is about $\mathcal{O}(8.3 \times 10^{-2})$ or so. A detailed list of sensitivities to all of these processes at individual and combined level is also presented in table 6 for convenience. The corresponding bound on $t \to ch$ as reported in ref. [19] and by the ATLAS [46, 47] and CMS [48] experiments are about 0.1 which is about one order of magnitude larger than the best bound obtained by us. This is partially due to the fact that in obtaining tch final state we do not restrict ourselves merely to the pair-production of $t\bar{t}$ unlike them. Thus in their study only diagrams of type figures 1 (a) and 1 (c) are relevant; in our case all three processes in Fig 1 occur. This translates into about 14 times larger cross-section for us compared to $\sigma_{t\bar{t}} \times 2Br(t \to ch)$ as in their work too, the other top decays semileptonically as $t \to bl\nu_l$. Obviously, since in our case, one of the top-quarks decaying to ch or uh, can be off-shell, it results in a further advantage for us in terms of reconstruction efficiencies.

5.2 Projected sensitivities at the LHC-14

Guided with the aforementioned bounds as obtained from various final state topologies using the observed 7 and $8\,\mathrm{TeV}$ LHC data in the previous subsection, in this subsection we provide estimate for the forthcoming LHC run with $\sqrt{s} = 14\,\mathrm{TeV}$. As we have noticed above, the best bound on the $\sqrt{\xi_{tc}^2 + \xi_{tu}^2}$ correspond to the $pp \to l^\pm + 3j + b-\mathrm{jet} + \not{E}_T$ detection mode. We will therefore focus on this particular detection mode itself.

Using `MadGraph5`, we find the bare cross-section for the production-process responsible for the aforementioned topology, $pp \to tch$, at $\sqrt{s} = 14\,\mathrm{TeV}$ to be $431.5\xi_{tc}^2 + 441.2\xi_{tu}^2$ pb, which is about a factor of 4 larger compared to at $8\,\mathrm{TeV}$, see table 2. This in the ideal case assuming a full reconstruction of the tch and in the absence of any SM background yields, $\sqrt{\xi_{tc}^2 + \xi_{tu}^2} \lesssim 0.15 \times 10^{-3}$ for an integrated luminosity $100\,\mathrm{fb}^{-1}$.

The cross-sections for the relevant SM processes which contribute to the background to our final-state are estimated to be, 6.01 (2.91) fb, 1.29 (0.59) fb, and, 1161.3 pb for $pp \to t\bar{b}Z(\bar{t}bZ)$, $pp \to t\bar{b}h(\bar{t}bh)$, and, $pp \to t\bar{t} + nj; n \leq 3$ respectively. This, using the exact same cuts as mentioned in the previous subsection, and, the demand that the two jets reconstruct to a Higgs-Boson, and, the only lepton in our final state reconstruct to a top-quark when paired with the b-jet and the missing transverse energy, in our final state, translates into a net SM background of $2.18\,\mathrm{fb}$ for the final state under consideration. Thus from our complete analysis, we obtain $\sqrt{\xi_{tc}^2 + \xi_{tu}^2} \lesssim 1.39\ (1.06) \times 10^{-3}$ for $\int \mathcal{L}dt = 100\ (300)\,\mathrm{fb}^{-1}$. It is to be noted that this is better only by a factor of about 2.7 compared to the bound obtained using the $8\,\mathrm{TeV}$ data for the same signatures, while one naively expect it to be better by a factor of four. The reason behind this is that for 7 and $8\,\mathrm{TeV}$ data, the SM background was not so significant and therefore the criterion that the number of observed signal events should not exceed one turn out to be stronger while for $14\,\mathrm{TeV}$ case it was actually $S/\sqrt{B}$ criterion which ruled over the former in estimating projected LHC sensitivities on the FCNC couplings.

– 11 –

6 Conclusions

We have studied the flavor-changing couplings of the Higgs boson with the top-quark in light of the Higgs discovery, using the data at the LHC, for both $\sqrt{s} = 7\,\text{TeV}$ and 8 TeV, along with the Tevatron measurements of the total decay width of the top-quark. In order to obtain better bounds to these processes we studied the same-sign top pair production, $pp \rightarrow tt(\bar{t}\bar{t})$, single top production in association with a light parton jet, $pp \rightarrow t\bar{j}(\bar{t}j)$, and the process where the single top-quark is produced in association with a Higgs and a light parton jet, $pp \rightarrow t\bar{j}h(\bar{t}jh)$. In our study, we found that the process $pp \rightarrow t\bar{j}h(\bar{t}jh)$ can be extremely useful in providing stronger bounds on the flavor-changing couplings of the order of 2.9×10^{-3}, particularly in case of the latter process with the Higgs-boson decays into a pair of jets and the (anti)top-quark decays semileptonically into a b-jet, a lepton and an invisible neutrino using the full data at $\sqrt{s} = 8$ TeV. To put things in perspective, we mention in passing that these constraints are significantly better than the one obtained from top decays, following pair production of tops, and also single top production [49]. Our sensitivities on $\sqrt{\xi_{tc}^2 + \xi_{tu}^2}$ are complementary to the one obtained by the low energy experiments through the D0-oscillations [49] on the product $|\xi_{tc}\xi_{tu}|$ as listed in table 3. Note that the latter product alone is not sufficient particularly when one of the FCNC-couplings becomes very small or is simply zero. Our estimates for the 14 TeV LHC suggest that the sensitivities can be improved just a bit more to 1.1×10^{-3} with $300\,\text{fb}^{-1}$ data.

We also note that although the sensitivities on FCNCs are better by a factor of about 1.8 for the process (c) in the $h \rightarrow 2\,jets$ detection mode compared to $h \rightarrow b\bar{b}$, due to its relatively clean signature the latter can still be quite useful to constrain the FCNCs. This, therefore confirms that it is highly desirable to tag b's for achieving better sensitivities on the FCNC couplings considered in this paper. Note also that in principle these can be further improved by a factor of two or so provided the produced top-quark and the Higgs-boson could be reconstructed fully. Therefore it is worthwhile for the ATLAS and CMS collaborations to consider possible ways of full reconstruction to further constrain the crucially important flavor-changing couplings of the Higgs-boson.

S. No.	Observable	2σ sensitivity for $\sqrt{a\xi_{tc}^2 + \xi_{tu}^2}$	
(1)	Γ_t	1.3	
(2)	$\mathcal{R}_{gg\gamma\gamma}$	1.7	
(3)	$\mathcal{R}_{gg2l2\nu}$	3.3	
(4)	$\mathcal{R}_{gg4l}$	1.8	
(5)	(2) + (3) + (4)	1.2	
		LHC-specific	
		$\sqrt{s} = 7\,TeV,\ \int \mathcal{L}dt = 5\,fb^{-1}$	$\sqrt{s} = 8\,TeV,\ \int \mathcal{L}dt = 22\,fb^{-1}$
(6)	$pp \longrightarrow tt(\bar{t}\bar{t})$	0.4	0.2
(7)	$pp \longrightarrow tj(\bar{t}j)$	2	1.3
(8)	$pp \longrightarrow tjh(\bar{t}jh)$	2.8×10^{-3}	1×10^{-3}
(9)	$pp \longrightarrow tt(\bar{t}\bar{t}), t \to bl\nu_l$	0.8	0.4
(10)	$pp \longrightarrow tj(\bar{t}j), t \to bl\nu_l$	3.2	1.9
(11)	$pp \longrightarrow tjh(\bar{t}jh), t \to bl\nu_l, h \to b\bar{b}$	13×10^{-3}	5×10^{-3}
(12)	$pp \longrightarrow tjh(\bar{t}jh), t \to bl\nu_l, h \to \gamma\gamma$	20.6×10^{-2}	8.3×10^{-2}
(13)	$pp \longrightarrow tjh(\bar{t}jh), t \to bl\nu_l, h \to jj$	7.3×10^{-3}	2.9×10^{-3}
(14)	(1) + (5) + (6)	0.4	0.2
(15)	(1) + (5) + (7)	0.9	0.9
(16)	(1) + (5) + (8)	2.8×10^{-3}	1×10^{-3}
(17)	(1) + (5) + (9)	0.8	0.4
(18)	(1) + (5) + (10)	0.9	0.9
(19)	(1) + (5) + (11)	13×10^{-3}	5×10^{-3}
(20)	(1) + (5) + (12)	20.6×10^{-2}	8.3×10^{-2}
(21)	(1) + (5) + (13)	7.3×10^{-3}	2.9×10^{-3}

Table 6. Upper bounds on the $|a\xi_{tc}^2 + \xi_{tu}^2|^{1/2}$ at the 2σ level from various observations. $a = 0.08$ for the cases with same-sign top pair in S. Nos. (6), (9), (14) and (17) while $a = 1$ for all other cases.

A Composition of $pp \longrightarrow t\bar{q}_u(\bar{t}q_u)$ where $q_u = \{u, c\}$

A.1 For $\sqrt{s} = 7$ TeV

$$
\begin{aligned}
\sigma_{pp\to tc+t\bar{c}} &= \sigma_{cctc} + \sigma_{c\bar{c}t\bar{c}} + \sigma_{uctc} + \sigma_{u\bar{c}t\bar{c}} \\
&\quad + \mathcal{P}_{b\to c}\left(\sigma_{bctb} + \sigma_{c\bar{b}t\bar{b}} + \sigma_{butb} + \sigma_{u\bar{b}t\bar{b}}\right) + \sigma_{b\bar{b}t\bar{c}} + \sigma_{ggt\bar{c}} \\
&= (20.83 + 0.48 P_{b\to q_u})\xi_{tc}^2 + (1.26 + 6.96 P_{b\to q_u})\xi_{tu}^2 \ \text{fb} \\
&= 21.03\xi_{tc}^2 + 4.18\xi_{tu}^2 \ \text{fb}
\end{aligned} \tag{A.1}
$$

$$
\begin{aligned}
\sigma_{pp\to \bar{t}c+\bar{t}\bar{c}} &= \sigma_{c\bar{c}\bar{t}c} + \sigma_{\bar{c}\bar{c}\bar{t}\bar{c}} + \sigma_{\bar{u}c\bar{t}c} + \sigma_{\bar{u}\bar{c}\bar{t}\bar{c}} \\
&\quad + \mathcal{P}_{b\to c}\left(\sigma_{b\bar{c}\bar{t}b} + \sigma_{\bar{c}\bar{b}\bar{t}\bar{b}} + \sigma_{b\bar{u}\bar{t}b} + \sigma_{\bar{u}\bar{b}\bar{t}\bar{b}}\right) + \sigma_{b\bar{b}\bar{t}c} + \sigma_{gg\bar{t}c} \\
&= (20.83 + 0.48 P_{b\to q_u})\xi_{tc}^2 + (0.2 + 1.02 P_{b\to q_u})\xi_{tu}^2 \ \text{fb} \\
&= 21.03\xi_{tc}^2 + 0.63\xi_{tu}^2 \ \text{fb}
\end{aligned} \tag{A.2}
$$

$$
\begin{aligned}
\sigma_{pp\to tu+t\bar{u}} &= \sigma_{cutu} + \sigma_{c\bar{u}t\bar{u}} + \sigma_{uutu} + \sigma_{u\bar{u}t\bar{u}} \\
&\quad + \mathcal{P}_{b\to u}\left(\sigma_{bctb} + \sigma_{c\bar{b}t\bar{b}} + \sigma_{butb} + \sigma_{u\bar{b}t\bar{b}}\right) + \sigma_{b\bar{b}t\bar{u}} + \sigma_{ggt\bar{u}}
\end{aligned}
$$

$$= (3.91 \times 10^{-6} + 0.48 P_{b \to q_u}) \xi_{tc}^2 + (20.6 + 6.96 P_{b \to q_u}) \xi_{tu}^2 \ \text{fb}$$
$$= 0.2 \xi_{tc}^2 + 23.52 \xi_{tu}^2 \ \text{fb} \tag{A.3}$$

$$\sigma_{pp \to \bar{t}u + t\bar{u}} = \sigma_{u\bar{c}\bar{t}u} + \sigma_{\bar{u}\bar{c}\bar{t}\bar{u}} + \sigma_{\bar{u}u\bar{t}u} + \sigma_{\bar{u}\bar{u}\bar{t}\bar{u}}$$
$$+ \mathcal{P}_{b \to u} \left(\sigma_{b\bar{c}\bar{t}b} + \sigma_{\bar{c}\bar{b}\bar{t}\bar{b}} + \sigma_{b\bar{u}\bar{t}b} + \sigma_{\bar{u}\bar{b}\bar{t}\bar{b}} \right) + \sigma_{b\bar{b}\bar{t}u} + \sigma_{gg\bar{t}u}$$
$$= (3.91 \times 10^{-6} + 0.48 P_{b \to q_u}) \xi_{tc}^2 + (20.6 + 1.02 P_{b \to q_u}) \xi_{tu}^2 \ \text{fb}$$
$$= 0.2 \xi_{tc}^2 + 21.03 \xi_{tu}^2 \ \text{fb} \tag{A.4}$$

Here we have assumed $P_{b \to q_u} = 0.42$.

A.2 For $\sqrt{s} = 8$ TeV

$$\sigma_{pp \to tc + t\bar{c}} = \sigma_{cctc} + \sigma_{c\bar{c}t\bar{c}} + \sigma_{uctc} + \sigma_{u\bar{c}t\bar{c}}$$
$$+ \mathcal{P}_{b \to c} \left(\sigma_{bctb} + \sigma_{\bar{c}\bar{b}t\bar{b}} + \sigma_{butb} + \sigma_{u\bar{b}t\bar{c}} \right) + \sigma_{b\bar{b}t\bar{c}} + \sigma_{ggt\bar{c}}$$
$$= (29.56 + 0.68 P_{b \to q_u}) \xi_{tc}^2 + (1.54 + 8.48 P_{b \to q_u}) \xi_{tu}^2 \ \text{fb}$$
$$= 29.85 \xi_{tc}^2 + 5.1 \xi_{tu}^2 \ \text{fb} \tag{A.5}$$

$$\sigma_{pp \to \bar{t}c + t\bar{c}} = \sigma_{c\bar{c}\bar{t}c} + \sigma_{\bar{c}\bar{c}\bar{t}\bar{c}} + \sigma_{\bar{u}c\bar{t}c} + \sigma_{\bar{u}\bar{c}\bar{t}\bar{c}}$$
$$+ \mathcal{P}_{b \to c} \left(\sigma_{b\bar{c}\bar{t}b} + \sigma_{\bar{c}\bar{b}\bar{t}\bar{b}} + \sigma_{b\bar{u}\bar{t}b} + \sigma_{\bar{u}\bar{b}\bar{t}\bar{b}} \right) + \sigma_{b\bar{b}\bar{t}c} + \sigma_{gg\bar{t}c}$$
$$= (29.56 + 0.68 P_{b \to q_u}) \xi_{tc}^2 + (0.28 + 1.4 P_{b \to q_u}) \xi_{tu}^2 \ \text{fb}$$
$$= 29.85 \xi_{tc}^2 + 0.34 \xi_{tu}^2 \ \text{fb} \tag{A.6}$$

$$\sigma_{pp \to tu + t\bar{u}} = \sigma_{cutu} + \sigma_{c\bar{u}t\bar{u}} + \sigma_{uutu} + \sigma_{u\bar{u}t\bar{u}}$$
$$+ \mathcal{P}_{b \to u} \left(\sigma_{bctb} + \sigma_{\bar{c}\bar{b}t\bar{b}} + \sigma_{butb} + \sigma_{u\bar{b}t\bar{b}} \right) + \sigma_{b\bar{b}t\bar{u}} + \sigma_{ggt\bar{u}}$$
$$= (4.89 \times 10^{-6} + 0.66 P_{b \to q_u}) \xi_{tc}^2 + (29.26 + 0.66 P_{b \to q_u}) \xi_{tu}^2 \ \text{fb}$$
$$= 0.32 \xi_{tc}^2 + 29.54 \xi_{tu}^2 \ \text{fb} \tag{A.7}$$

$$\sigma_{pp \to \bar{t}u + t\bar{u}} = \sigma_{u\bar{c}\bar{t}u} + \sigma_{\bar{u}\bar{c}\bar{t}\bar{u}} + \sigma_{\bar{u}u\bar{t}u} + \sigma_{\bar{u}\bar{u}\bar{t}\bar{u}}$$
$$+ \mathcal{P}_{b \to u} \left(\sigma_{b\bar{c}\bar{t}b} + \sigma_{\bar{c}\bar{b}\bar{t}\bar{b}} + \sigma_{b\bar{u}\bar{t}b} + \sigma_{\bar{u}\bar{b}\bar{t}\bar{b}} \right) + \sigma_{b\bar{b}\bar{t}u} + \sigma_{gg\bar{t}u}$$
$$= (4.87 \times 10^{-6} + 0.68 P_{b \to q_u}) \xi_{tc}^2 + (29.26 + 1.4 P_{b \to q_u}) \xi_{tu}^2 \ \text{fb}$$
$$= 0.29 \xi_{tc}^2 + 30.13 \xi_{tu}^2 \ \text{fb} \tag{A.8}$$

References

[1] ATLAS collaboration, *Observation of a new particle in the search for the standard model Higgs boson with the ATLAS detector at the LHC*, *Phys. Lett.* **B 716** (2012) 1 [arXiv:1207.7214] [INSPIRE].

[2] CMS collaboration, *Observation of a new boson at a mass of* 125 *GeV with the CMS experiment at the LHC*, *Phys. Lett.* **B 716** (2012) 30 [arXiv:1207.7235] [INSPIRE].

[3] ATLAS collaboration, *Combined measurements of the mass and signal strength of the Higgs-like boson with the ATLAS detector using up to 25 fb^{-1} of proton-proton collision data*, [ATLAS-CONF-2013-014](#) (2013).

[4] CMS collaboration, *Properties of the Higgs-like boson in the decay $H \to ZZ \to 4l$ in pp collisions at $\sqrt{s} = 7$ and 8 TeV*, [CMS-PAS-HIG-13-002](#) (2013).

[5] K. Agashe, G. Perez and A. Soni, *Flavor structure of warped extra dimension models*, [*Phys. Rev.* **D 71** (2005) 016002](#) [[hep-ph/0408134](#)] [[INSPIRE](#)].

[6] K. Agashe, G. Perez and A. Soni, *Collider signals of top quark flavor violation from a warped extra dimension*, [*Phys. Rev.* **D 75** (2007) 015002](#) [[hep-ph/0606293](#)] [[INSPIRE](#)].

[7] M. Blanke, A.J. Buras, B. Duling, S. Gori and A. Weiler, *$\Delta F = 2$ observables and fine-tuning in a warped extra dimension with custodial protection*, [*JHEP* **03** (2009) 001](#) [[arXiv:0809.1073](#)] [[INSPIRE](#)].

[8] M. Blanke, A.J. Buras, B. Duling, K. Gemmler and S. Gori, *Rare K and B decays in a warped extra dimension with custodial protection*, [*JHEP* **03** (2009) 108](#) [[arXiv:0812.3803](#)] [[INSPIRE](#)].

[9] S. Casagrande, F. Goertz, U. Haisch, M. Neubert and T. Pfoh, *Flavor physics in the Randall-Sundrum model: I. Theoretical setup and electroweak precision tests*, [*JHEP* **10** (2008) 094](#) [[arXiv:0807.4937](#)] [[INSPIRE](#)].

[10] K. Agashe and R. Contino, *Composite Higgs-mediated FCNC*, [*Phys. Rev.* **D 80** (2009) 075016](#) [[arXiv:0906.1542](#)] [[INSPIRE](#)].

[11] A. Azatov, M. Toharia and L. Zhu, *Higgs mediated FCNC'S in warped extra dimensions*, [*Phys. Rev.* **D 80** (2009) 035016](#) [[arXiv:0906.1990](#)] [[INSPIRE](#)].

[12] M. Bauer, S. Casagrande, U. Haisch and M. Neubert, *Flavor physics in the Randall-Sundrum model: II. Tree-level weak-interaction processes*, [*JHEP* **09** (2010) 017](#) [[arXiv:0912.1625](#)] [[INSPIRE](#)].

[13] B. Keren-Zur et al., *On partial compositeness and the CP asymmetry in charm decays*, [*Nucl. Phys.* **B 867** (2013) 394](#) [[arXiv:1205.5803](#)] [[INSPIRE](#)].

[14] T.P. Cheng and M. Sher, *Mass matrix ansatz and flavor nonconservation in models with multiple Higgs doublets*, [*Phys. Rev.* **D 35** (1987) 3484](#) [[INSPIRE](#)].

[15] M.E. Luke and M.J. Savage, *Flavor changing neutral currents in the Higgs sector and rare top decays*, [*Phys. Lett.* **B 307** (1993) 387](#) [[hep-ph/9303249](#)] [[INSPIRE](#)].

[16] D. Atwood, L. Reina and A. Soni, *Phenomenology of two Higgs doublet models with flavor changing neutral currents*, [*Phys. Rev.* **D 55** (1997) 3156](#) [[hep-ph/9609279](#)] [[INSPIRE](#)].

[17] P.M. Aquino, G. Burdman and O.J.P. Eboli, *A signal for a theory of flavor at the LHC*, [*Phys. Rev. Lett.* **98** (2007) 131601](#) [[hep-ph/0612055](#)] [[INSPIRE](#)].

[18] N. Craig et al., *Searching for $t \to ch$ with multi-leptons*, [*Phys. Rev.* **D 86** (2012) 075002](#) [[arXiv:1207.6794](#)] [[INSPIRE](#)].

[19] K.-F. Chen, W.-S. Hou, C. Kao and M. Kohda, *When the Higgs meets the top: search for $t \to ch^0$ at the LHC*, [*Phys. Lett.* **B 725** (2013) 378](#) [[arXiv:1304.8037](#)] [[INSPIRE](#)].

[20] C. Zhang and F. Maltoni, *Top-quark decay into Higgs boson and a light quark at next-to-leading order in QCD*, [*Phys. Rev.* **D 88** (2013) 054005](#) [[arXiv:1305.7386](#)] [[INSPIRE](#)].

[21] M. Jezabek and J.H. Kuhn, *QCD corrections to semileptonic decays of heavy quarks*, *Nucl. Phys.* **B 314** (1989) 1 [ɪɴSPIRE].

[22] PARTICLE DATA GROUP collaboration, J. Beringer et al., *Review of particle physics*, *Phys. Rev.* **D 86** (2012) 010001 [ɪɴSPIRE].

[23] A. Belyaev, N.D. Christensen and A. Pukhov, *CalcHEP 3.4 for collider physics within and beyond the standard model*, *Comput. Phys. Commun.* **184** (2013) 1729 [arXiv:1207.6082] [ɪɴSPIRE].

[24] D. Atwood, S.K. Gupta and A. Soni, *Same-sign tops: a powerful diagnostic test for models of new physics*, *JHEP* **04** (2013) 035 [arXiv:1301.2250] [ɪɴSPIRE].

[25] E.L. Berger, Q.-H. Cao, C.-R. Chen, C.S. Li and H. Zhang, *Top quark forward-backward asymmetry and same-sign top quark pairs*, *Phys. Rev. Lett.* **106** (2011) 201801 [arXiv:1101.5625] [ɪɴSPIRE].

[26] C. Degrande, J.-M. Gerard, C. Grojean, F. Maltoni and G. Servant, *An effective approach to same sign top pair production at the LHC and the forward-backward asymmetry at the Tevatron*, *Phys. Lett.* **B 703** (2011) 306 [arXiv:1104.1798] [ɪɴSPIRE].

[27] J.A. Aguilar-Saavedra and M. Pérez-Victoria, *No like-sign tops at Tevatron: constraints on extended models and implications for the $t\bar{t}$ asymmetry*, *Phys. Lett.* **B 701** (2011) 93 [arXiv:1104.1385] [ɪɴSPIRE].

[28] S.K. Gupta, *Same sign top-pairs in a non-universal Z' model at the LHC*, arXiv:1011.4960 [ɪɴSPIRE].

[29] F. Hubaut, *Latest ATLAS studies on Higgs to diboson states*, talk given at the *Rencontres de Moriond*, March 2–9, La Thuile, Italy (2013).

[30] ATLAS collaboration, *Measurements of the properties of the Higgs-like boson in the two photon decay channel with the ATLAS detector using $25\,fb^{-1}$ of proton-proton collision data*, ATLAS-CONF-2013-012 (2013).

[31] CMS collaboration, *Updated measurements of the Higgs boson at 125 GeV in the two photon decay channel*, CMS-PAS-HIG-13-001 (2013).

[32] C. Ochando, *Study of Higgs production in bosonic decays channels in CMS*, talk given at the *Rencontres de Moriond*, March 2–9, La Thuile, Italy (2013).

[33] E. Mountricha, *Study of Higgs production in bosonic decay channels at ATLAS*, talk given at the *Rencontres de Moriond*, March 2–9, La Thuile, Italy (2013).

[34] ATLAS collaboration, *Measurements of the properties of the Higgs-like boson in the $WW^{(*)} \to \ell\nu\ell\nu$ decay channel with the ATLAS detector using $25\,fb^{-1}$ of proton-proton collision data*, ATLAS-CONF-2013-030 (2013).

[35] G. Gómez-Ceballos, *Study of standard model scalar production in bosonic decay channels in CMS*, talk given at the *Rencontres de Moriond*, March 2–9, La Thuile, Italy (2013).

[36] CMS collaboration, *Evidence for a particle decaying to W^+W^- in the fully leptonic final state in a standard model Higgs boson search in pp collisions at the LHC*, CMS-PAS-HIG-13-003 (2013).

[37] ATLAS collaboration, *Measurements of the properties of the Higgs-like boson in the four lepton decay channel with the ATLAS detector using $25\,fb^{-1}$ of proton-proton collision data*, ATLAS-CONF-2013-013 (2013).

[38] CMS collaboration, *Properties of the Higgs-like boson in the decay $H \to ZZ \to 4l$ in pp collisions at $\sqrt{s} = 7$ and 8 TeV*, CMS-PAS-HIG-13-002 (2013).

[39] UTFIT collaboration, M. Bona et al., *Model-independent constraints on $\Delta F = 2$ operators and the scale of new physics*, *JHEP* **03** (2008) 049 [arXiv:0707.0636] [InSPIRE].

[40] T. Stelzer and W.F. Long, *Automatic generation of tree level helicity amplitudes*, *Comput. Phys. Commun.* **81** (1994) 357 [hep-ph/9401258] [InSPIRE].

[41] J. Alwall et al., *MadGraph/MadEvent v4: the new web generation*, *JHEP* **09** (2007) 028 [arXiv:0706.2334] [InSPIRE].

[42] J. Alwall, M. Herquet, F. Maltoni, O. Mattelaer and T. Stelzer, *MadGraph 5: going beyond*, *JHEP* **06** (2011) 128 [arXiv:1106.0522] [InSPIRE].

[43] J. Pumplin et al., *New generation of parton distributions with uncertainties from global QCD analysis*, *JHEP* **07** (2002) 012 [hep-ph/0201195] [InSPIRE].

[44] D. Stump et al., *Inclusive jet production, parton distributions and the search for new physics*, *JHEP* **10** (2003) 046 [hep-ph/0303013] [InSPIRE].

[45] ATLAS collaboration, *ATLAS: detector and physics performance technical design report*, CERN-LHCC-99-14 (1999).

[46] ATLAS collaboration, *Search for flavor-changing neutral currents in $t \to cH$, with $H \to \gamma\gamma$ and limit on the tcH coupling*, ATLAS-CONF-2013-081 (2013).

[47] ATLAS collaboration, *Search for top quark decays $t \to qH$ with $H \to \gamma\gamma$ using the ATLAS detector*, *JHEP* **06** (2014) 008 [arXiv:1403.6293] [InSPIRE].

[48] CMS Collaboration, *A search for anomalous production of events with three or more leptons using 19.5/fb of $\sqrt{s} = 8$ TeV LHC data*, CMS-PAS-SUS-13-002 (2013).

[49] R. Harnik, J. Kopp and J. Zupan, *Flavor violating Higgs decays*, *JHEP* **03** (2013) 026 [arXiv:1209.1397] [InSPIRE].